

# Docking Performance Against Turbidity Using Active Marker Under Day and Night Environment

Khin Nwe Lwin<sup>1</sup>, Myo Myint<sup>1</sup>, Naoki Mukada<sup>1</sup>, Daiki Yamada<sup>1</sup>, Takayuki Matsuno<sup>1</sup>, and Mamoru Minami<sup>1</sup>

<sup>1</sup>Graduate School of Natural Science and Technology, Okayama University, Japan  
(Tel: 81-86-251-8233, Fax: 81-86-251-8233)  
<sup>1</sup>pceo8sjx@s.okayama-u.ac.jp

**Abstract:** Nowadays, Autonomous Underwater Vehicle (AUV) is playing an important role for human society in different applications such as inspection of underwater structures (dams, bridges). We have developed a stereo-vision based docking approach for underwater battery recharging to enable the AUV to operate for extended periods without returning surface vehicle for recharging. Since underwater battery recharging units are supposed to be installed in deep sea, the deep-sea docking experiments cannot avoid turbidity and low light environment. In this study, the proposed system with a newly designed an active 3D marker have been developed to improve the performance of the proposed system especially in turbid water. We conducted experiments to verify the robustness of the proposed docking approach in a simulated pool where lighting changes from day to night and the water is turbid. The experimental results have confirmed the robustness of the proposed docking system against turbidity and illumination variation.

**Keywords:** Visual Servoing, active marker, underwater docking, stereo vision, turbidity, illumination variation

## 1 INTRODUCTION

Japan has many areas of sea from which future resources can be taken out using advanced technologies. Autonomous Underwater Vehicle (AUV) plays an important role in deep sea works such as oil pipe inspection, survey of sea floor, searching expensive metal, etc [1]-[4]. Japan government is now seriously considering searching methane hydrate as future energy solution. To do such novel works that takes long period in deep sea, one of the main limitation of AUVs is limited power capacity. To solve this problem, underwater battery recharging unit with a docking function is one of the solutions to extend the operation time of AUVs. Several approaches using different sensors have been conducted worldwide for underwater docking operation [5]-[6]. Normally, long navigation is performed using acoustic sensors and camera vision is used for final step of docking process. Vision-based navigation is one of the dominant positioning units especially high accuracy is essential. Vision based system can be integrated with other sensor units.

Most of the studies related to vision based navigation for underwater vehicle are based on single camera [7]-[9]. Apart from them, we have developed a stereo-vision based docking approach for AUV [10]-[13]. In our approach, the relative pose between the underwater vehicle and a known 3D marker is estimated using Real-time Multi-step GA (RM-GA) that is real-time 3D pose estimation method. Avoiding the disadvantages of features based recognition methods that are based on 2D to 3D reconstruction, 3D model based matching method is used that is based on 3D to 2D projection method in our approach. One of the main drawbacks of 2D-to-3D re-

construction is incorrectly mapping between corresponding points in images.

Since underwater environment is more complex than space and ground, there are many disturbances for vision-based underwater vehicles. Therefore, it is important to consider the possible disturbances before testing the proposed approach in the sea. The common disturbances for vision-based underwater vehicle are light environment and turbidity. Since underwater battery recharging units are supposed to be installed in deep sea to save the time consuming and work done from human beings in the case of returning surface vehicle for recharging, the deep-sea docking experiments cannot avoid turbidity and low light environment. According to the authors' knowledge, there is no study on docking system using stereo-vision based real-time visual servoing with performance tolerance of illumination and turbidity.

In this study, we newly designed an active 3D marker and used to improve the performance of the system especially in high turbidity. We conducted experiments to verify the robustness of the proposed docking approach in simulated pool where lighting changes from day to night and the turbidity of the water is high. The experimental results have confirmed the robustness of the docking system using stereo-vision based 3D pose estimation against turbidity and light changing.

The remainder of the paper is organized as follows: Section 2 describes the method of 3D pose estimation. Experiment results are reported in section 3 with discussion and conclude in section 4.

## 2 REMOTELY OPERATED VEHICLE

Hovering type underwater vehicle (manufactured by Kowa cooperation) is used as a test bed as shown in Fig.1. Two fixed cameras installed at the front of the vehicle are used for real time pose tracking. In thruster unit, four thrusters with maximum thrust force of 4.9[N] each are controlled to move the vehicle along desired path. The vehicle can dive up to 50 [m] and two LED light sources are also installed on the vehicle.

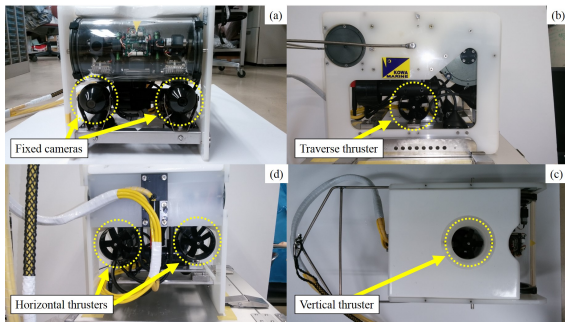


Fig. 1. Photograph of ROV (a) front view showing two cameras, (b) side view showing traverse thruster, (c) back view showing horizontal thrusters, and (d) top view showing vertical thruster.

## 3 3D MOVING ON SENSING (MOS) USING REAL-TIME MULTI-STEP GA

In previous study [10], we introduced 3D MoS that uses three dimensional measurement with solid object recognition based on visual servoing technology. In this system, RM-GA is used to estimate the relative pose between the vehicle and a known 3D marker. Here, we will discuss on 3D pose estimation using RM-GA briefly for background of readers.

Figure 2 shows the model-based matching method using dual-eye cameras for 3D pose estimation. In Fig. 2,  $\Sigma_{CR}$  and  $\Sigma_{CL}$  are the reference coordinate frame of the right camera and the left camera.  $\Sigma_H$  is the reference frame of the ROV.  $\Sigma_M$  is the reference frame of the real target object. The solid model of the real target object in space is projected naturally to the dual-eyes cameras images and the dotted 3D marker model, where the pose is given by one of GA's genes, is projected from 3D to 2D. The different relative pose is calculated by comparing the projected 2D image and the solid model captured by the dualeye cameras. Finally, the best model of the target object that represents the true pose can be obtained based on its highest fitness value. The fitness function is constructed to evaluate the matching degree between the projected model and the captured image. Detailed explanation about the fitness function is referred to our previous paper [14].

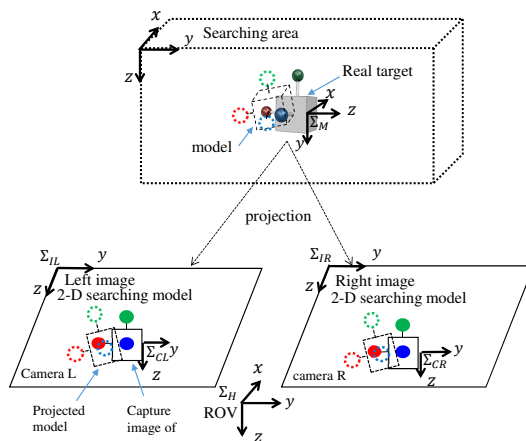


Fig. 2. Model-based matching method using dual-eye cameras and 3D marker. A solid object in 3D space is real target and dotted ones in 3D and 2D space are models that are predefined in 3D space and projected to 2D left and right images.

### 3.1 Real-time Multi-step GA

In the proposed 3D model-based recognition method, searching for all possible models is time consuming for real-time recognition. Therefore, the problem of finding/recognizing the 3D marker and detecting its pose is converted into an optimization problem with a multi-peak distribution. The genetic algorithm is used and utilized as RM-GA to estimate the relative pose between the ROV and 3D marker. Figure. 3 shows the flowchart of the RM-GA. Position and orientation of the three-dimensional model are represented as individual of the chromosome. The former 36 bits represent the position of the 3D marker and the later 36 bits describe the orientation defined by a quaternion.

Firstly, a random population of the chromosome is generated. A new pair of left and right images is input. The RM-GA procedure is performed within 33 ms. The RM-GA find repeatedly the solutions to get the best pose of the target object within the video frame rate to deal with time varying distribution for newly input images. The fitness function is designed to get the maximum value when the model and the real target exactly coincide. The true pose of the target object is expressed with the peak of the mountain shape in the fitness distribution. Finally, the best pose of the individual can be made to approach the real target's pose. Although the pose of the target object is evaluated in 2D, convergence occurs in 3D. For the next input, a new video image is used.

### 3.2 Controller

The proportional controller is used to control the vehicle. The four thrusters that are mounted on the underwater robot are controlled by sending the command voltage based on the feedback relative pose between the underwater robot and the object (xd[mm], yd[mm], zd[mm]). The block diagram of the control system is shown in Fig. 4. The control voltage of

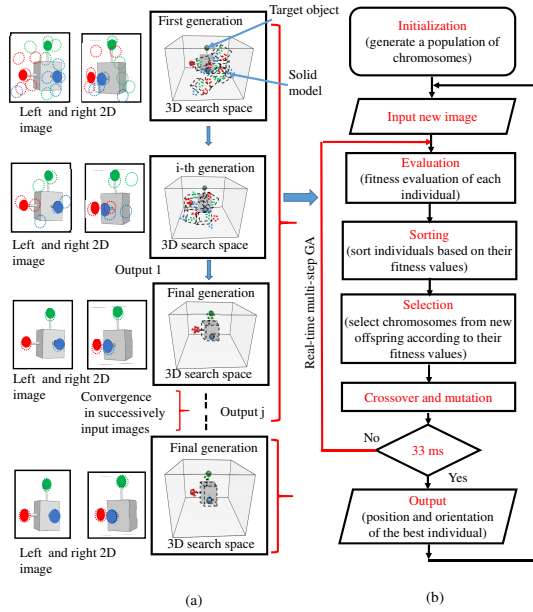


Fig. 3. Flowchart of the real-time multi-step GA: (a) the recognition process of the target pose is evaluated in 2D, convergence occurs in 3D (b) the flowchart of the RM-GA, the best solution is evaluated within 33 ms through the GA process.

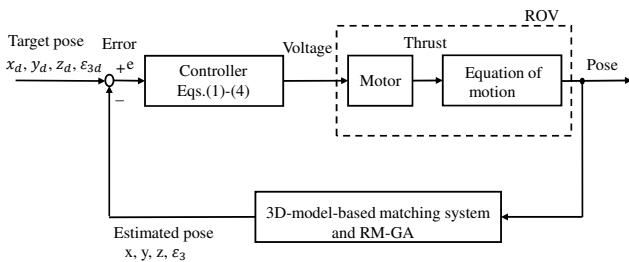


Fig. 4. Block Diagram of 3D MoS for Visual servoing based underwater vehicle.

the four thrusters is controlled as the following equations.

$$\text{The depth direction} : v_1 = k_{p1}(x_d - x) + 2.5 \quad (1)$$

$$\text{Vertical axis rotation} : v_2 = k_{p2}(\epsilon_{3d} - \epsilon_3) + 2.5 \quad (2)$$

$$\text{Vertical direction} : v_3 = k_{p3}(z_d - z) + 2.5 \quad (3)$$

$$\text{Horizontal direction} : v_4 = k_{p4}(y_d - y) + 2.5 \quad (4)$$

Where  $v_1, v_3$  and  $v_4$  are the control voltage of the four thrusters of  $x, z, y$  direction respectively.  $x_d, y_d, z_d$  are the desired relative pose between the vehicle and the target.  $\epsilon_{3d}$  is the rotation direction around the  $z$ -axis and it is expressed as the value of  $v_2$ . According to the experimental result, the gain coefficient is adjusted to perform the best condition for visual servoing.

### 3.3 Active Marker

In our previous researches [10]-[13], the passive marker was used to conduct the experiment. In the present study,

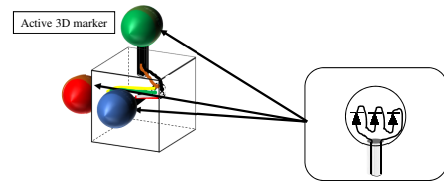


Fig. 5. Active 3D marker: Red, green and blue LED were installed into the white spherical ball and covered by colour balloon. The active marker was designed and constructed to improve the pose estimation at high turbidity level in day and night time. Figure 5 shows the appearance of the active marker. The circuit was created by combining the variable resistors, resistors, and the light emitting diodes such as red, green, and blue. The resistance value of the variable resistors, and the number of resistors are determined by trial and error. The 3D marker is constructed from a water proof box (100 mm × 100 mm × 100 mm) and the white spheres (diameter: 40 mm) are attached to the water proof box. The red, green and blue LED were installed into the white spherical ball and covered by the color balloon as shown in Fig. 5. This marker can be used as the passive marker when the light is switched off. The active marker allowed the ROV to recognize in day and night time by emitting the light of LED.

## 4 EXPERIMENTAL RESULTS AND DISCUSSION

### 4.1 3D Pose Estimation in Turbid Water

The 3D pose estimation was performed when the ROV and 3D marker were fixed with a distance of 600 mm between them under different turbidity levels in day and night time. The amount of turbidity is controlled by adding mud in water in the tank. Mud is chosen in order to simulate the natural condition. In this experiment, the turbidity level (Formazin Turbidity Unit, FTU) is measured by using a portable turbidity monitoring sensor (Model: TD-M500, manufactured by OPTEx).

The ROV performed visual servoing at about 600 mm in docking operation. It is the aware distance for docking operation to recognize the target object. Therefore, we give prominence to discuss 600 mm distance for recognition performance. Figure 6 shows the fitness value against turbidity using mud and the ROV and the 3D marker were fixed in distance 600 mm. The horizontal axis is described by the amount of mud ( $ml/m^3$ ) and the vertical axis is expressed in terms of fitness values and FTU values.

According to the results, the fitness value decreases from 1.3 to 0.1 in the case of day time and from 0.6 to 0.1 in the

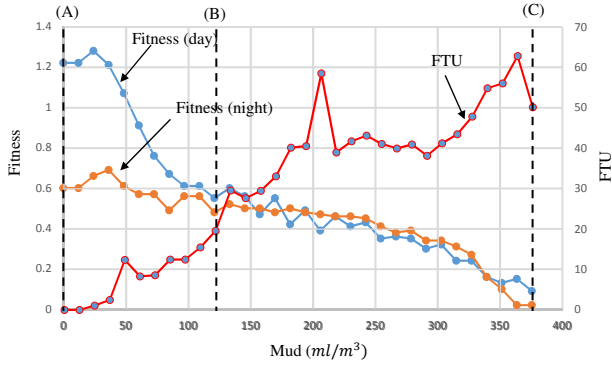


Fig. 6. Fitness values against turbidity at the distance 600 mm between the ROV and 3D marker. The illumination for day and night time are 1280 (lx) and 80 (lx) respectively. The left and right camera images taken at (A), (B), (C) are shown in Fig. 7.

case of night time when the turbidity is gradually increased from 0 FTU ( $0 \text{ ml/m}^3$ ) to 50.2 FTU ( $375.875 \text{ ml/m}^3$ ). The fitness value is nearly same at day and night time above 30 FTU. According to the experimental results, the performance of 3D pose estimation under different turbidity levels is analyzed and the maximum turbidity can be determined according to the defined threshold of fitness value. For example, when the ROV is controlled with the minimum fitness value of 0.4, the maximum turbidity is 40 FTU in that condition docking experiment can be conducted. To verify that concept, docking experiment in the pool in which turbidity is 40 was conducted under light changing environment. The detailed discussion on docking experiment is presented in the following section.

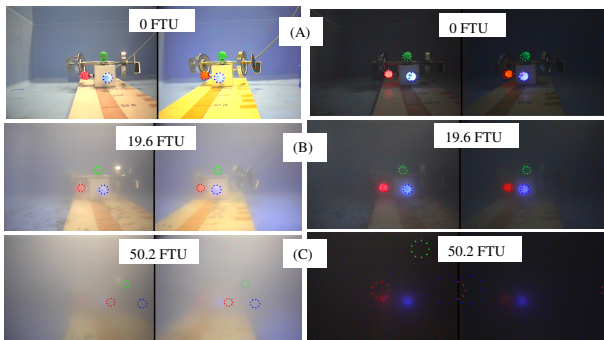


Fig. 7. Left and right images corresponding to the conditions of (A), (B), (C) in Fig.6 for day and night time. Dotted cycles mean recognized poses by RM-GA.

#### 4.2 Docking Performance Against Turbidity Under Changing Lighting Condition

This experiment was conducted in an indoor pool as shown in Fig. 8 in which the turbidity was created by adding mud (40 FTU). The desired pose ( $x_d = 600 \text{ mm}$  (350 mm for docking completion),  $y_d = 15 \text{ mm}$ ,  $z_d = -20 \text{ mm}$ , and  $\epsilon_{3d} =$

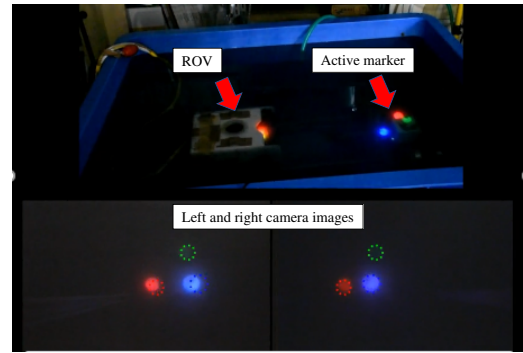


Fig. 8. Docking experiment in turbid water using an active marker under changing lighting environment.

0 deg) between the target and the ROV (see Fig. 9) is predefined so that the ROV performs docking by mean of visual servoing. The detailed explanation of docking strategy is referred to our previous study [10]. After the docking operation completed, the vehicle returned to a distance of 600 mm from the target in the x-direction for the next docking iteration.

The totally 17 times continuous docking was performed successfully by changing lighting from day time to night time as shown in Fig.10. Figure 10 shows the lighting simulation for each docking time. The horizontal direction is described by the number of docking times and the vertical direction is expressed with the illumination [Lx]. By adjusting the lighting condition, the maximum illumination is 1280 Lx in day time and minimum illumination is 80 Lx in night time. The illuminance was measured using a lux sensor (model: LX-1010B, manufactured by Milwaukee).

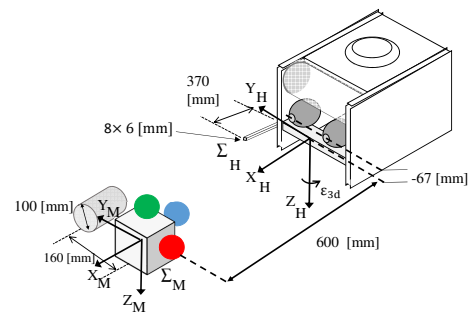


Fig. 9. Docking coordinate system.

The results of docking performance against turbidity at the maximum illumination 1280 Lx (day time) are shown in Fig. 11, and the results of docking performance at the minimum illumination 80 Lx are shown in Fig. 12. In Fig. 11 (a), the fitness value is above 0.8 for the few seconds of the recognition process and then increased to 1, which means that the system could recognize the 3D pose of the active marker well. Figures 11 (b), (c), (e), and (f) represent the relative pose between the desired pose and the estimated pose

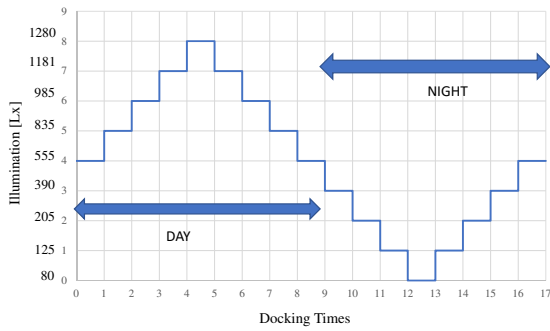


Fig. 10. Illumination simulated for each docking time. Lighting condition is changed from day time to night time gradually of the active marker recognized by RM-GA. Figure 11 (d) indicates the trajectory of the underwater robot based on  $\Sigma_H$  in Fig. 9 during the docking process.

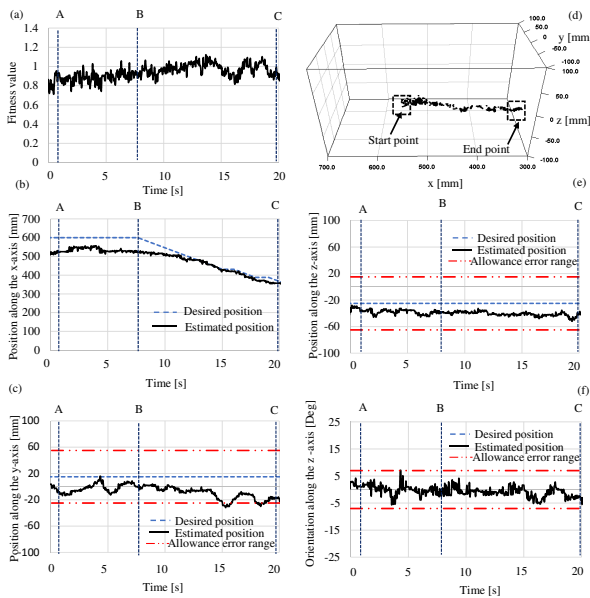


Fig. 11. Docking performance against turbidity (40 FTU) in the case of mud using dual-eye images recognition at 1280 Lx (maximum lighting condition): (a) fitness value, (b) position along the x-axis, (c) position along the y-axis, (d) 3D trajectory of the underwater vehicle, (e) position along the z-axis, and (f) orientation along the z-axis.

In docking strategy, visual servoing starts when the 3D marker is detected, which means the fitness value is above a defined threshold (0.4 in the present study). When the pose of the vehicle is within the allowable error range of  $\pm 40$  mm of the desired pose, as shown in Figs. 11(b), (c), and (e), and the orientation around the z-axis (f) is controlled to within 7 deg for the desired period (165 ms, which is equal to five times the control loop period) in this experiment, docking starts by decreasing the distance between the ROV and the 3D marker

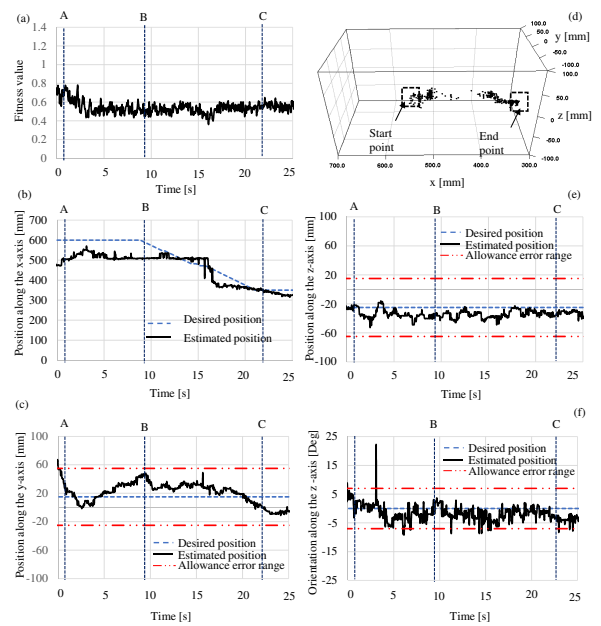


Fig. 12. Docking performance against turbidity (40 FTU) in the case of mud using dual-eye images recognition at 80 Lx (minimum lighting condition): (a) fitness value, (b) position along the x-axis, (c) position along the y-axis, (d) 3D trajectory of the underwater vehicle, (e) position along the z-axis, and (f) orientation along the z-axis.

from 550 mm to 350 mm, as shown in Fig. 11(b). The dotted line labeled “A” in each subfigure of Fig. 11 indicates the visual servoing state, where the desired position along the x-axis is 600 mm, and the desired position along the y-axis is within the allowance error range, as shown in Fig. 11(c). Visual servoing continues until the desired pose is within the error range for the y and z directions and the orientation around the z-axis, as shown in Figs. 11(c), (e), and (f). At time “B”, as shown in Figs. 11(b), (c), and (d), the docking criteria are satisfied and docking operation starts. Note that the position in the x direction at point “B” is approximately 500 mm because only the positions in the y and z directions and the orientation around the z-axis are considered in the docking criteria. The docking operation started approximately 7 s after starting the experiment. Finally, the docking operation was successfully completed approximately 20 s after starting the experiment. The dotted line labeled “C” in each subfigure of Fig. 11 indicates the state whereby the docking is completed.

In the case of 80 Lx (night time), the fitness value is about 0.8 in recognition of active 3D marker at the start of the experiment and then decreased to about 0.5 as shown in Fig. 12(a). The ROV could recognize the active marker even though the environment is dark. The desired position along the orientation around the z-axis are out of error range at 3 s as shown in Fig.12 (f). Therefore, visual servoing continues

until the desired pose of other direction  $y$ ,  $z$ , and orientation around the  $z$ -axis is within allowance error range. The time for docking from the start of the experiment is 25 s in this case. The underwater robot was confirmed to maintain the desired pose while docking was performed under changing lighting condition at high turbidity, as shown in Figs. 11 and 12(a) through (f). According to the experimental results, even though the lighting condition was changed from day to night in high turbidity, the relative pose of the 3D marker can keep recognize well and the docking has been done successfully against turbidity under changing lighting condition.

## 5 CONCLUSION

This paper presents the docking performance against turbidity of the proposed dual-eye based docking system using an active 3D marker under changing lighting condition. Pool docking experiment was conducted against turbidity using an ROV. Turbid water was simulated using mud taken from the real sea. Recognition performance against turbidity under day and night was verified in terms of fitness value that is used in the 3D pose estimation of RM-GA. 17 times continuously repeated docking in the turbid water was conducted and docking performance under day and night environment was discussed in details. The experimental results have confirmed the docking performance of the proposed system against turbidity under different lighting conditions. Docking experiment in the turbid sea under day and night environment will be conducted in future.

## ACKNOWLEDGMENT

This work is supported in part by KOWA corporation for the development of ROV.

## REFERENCES

- [1] Agbakwuru J. "Oil/Gas Pipeline Leak Inspection and Repair in Underwater Poor Visibility Conditions: Challenges and Perspectives," *Journal of Environmental Protection*, 2012.
- [2] Kume, A., Maki, T., Sakamaki, T. and Ura, T., "A method for obtaining high-coverage 3D images of rough seafloor using AUV-realtime quality evaluation and path-planning." *Journal of Robotics and Mechatronics*, 25(2), pp.364-374, 2013.
- [3] Ribas, D., Palomeras, N., Ridao, P., Carreras, M., Mallios, A., "Girona 500 auv: From survey to intervention." *IEEE/ASME Transactions on Mechatronics*, 17(1), pp.46-53, 2012.
- [4] Krupinski, S., Allibert, G., Hua, M.D. and Hamel, T., "Pipeline tracking for fully-actuated autonomous underwater vehicle using visual servo control." *In American Control Conference (ACC)*, pp.6196-6202. IEEE, 2012.
- [5] Son-Cheol Yu, Ura T., Fujii T. and Kondo H., "Navigation of autonomous underwater vehicles based on artificial underwater landmarks," *Proc. MTS/IEEE OCEANS Conf.*, vol.1, pp 409-416, 2001.
- [6] Steve Cowen, Susan Briest and James Dombrowski, "Underwater Docking of Autonomous Undersea Vehicle using Optical Terminal Guidance," *Proc. MTS/IEEE OCEANS Conf.*, vol.2, pp.1143-1147, 1997.
- [7] Eustice, R.M., Pizarro, O. and Singh, H., "Visually augmented navigation for autonomous underwater vehicles." *IEEE Journal of Oceanic Engineering*, 33(2), pp.103-122, 2008.
- [8] Jung, J., Choi, S., Choi, H.T. and Myung, H., "Localization of AUVs using depth information of underwater structures from a monocular camera." *In Ubiquitous Robots and Ambient Intelligence (URAI)*, 2016 13th International Conference, pp.444-446, IEEE, 2016.
- [9] Ghosh, S., Ray, R., Vadali, SR., Shome, SN., Nandy, S., "Reliable pose estimation of underwater dock using single camera: a scene invariant approach." *Machine Vision and Applications*, 27(2), pp. 221-36, 2016.
- [10] Myo Myint, Kenta Yonemori, Khin Nwe Lwin, Akira Yanou, Mamoru Minami. *J Intell Robot Syst (2017)*. DOI 10.1007/s10846-017-0703-6.
- [11] Myint, M., Yonemori, K., Yanou, A., Ishiyama, S., Minami, M., "Robustness of visual-servo against air bubble disturbance of underwater vehicle system using three-dimensional marker and dual-eye cameras." *In OCEANS 2015-MTS/IEEE*, pp.1-8, Washington DC, USA, 2015.
- [12] Myint, M., Yonemori, K., Yanou, A., Lwin, K. N., Minami, M., Ishiyama, S., "Visual servoing for underwater vehicle using dual-eyes evolutionary real-time pose tracking." *Journal of Robotics and Mechatronics*, 28(4), pp.543-558, 2016.
- [13] Myint, M., Yonemori, K., Yanou, A., Lwin, K.N., Minami, M. and Ishiyama, S., "Visual-based deep sea docking simulation of underwater vehicle using dual-eyes cameras with lighting adaptation." *In OCEANS 2016-Shanghai*, pp. 1-8, IEEE, 2016.
- [14] Song, W., Minami, M., Aoyagi, S., "On-line stable evolutionary recognition based on unit quaternion representation by motion-feedforward compensation." *International Journal of Intelligent Computing in Medical Sciences & Image Processing*, 2(2), pp.127-139, 2008.